

1 **Influence of African dust on tropical Atlantic coupled variability**

2
3 Amato T. Evan^{1,*}, Gregory R. Foltz², Dongxiao Zhang³, Daniel J. Vimont⁴

4 ¹University of Virginia, Department of Environmental Sciences, Charlottesville,
5 Virginia

6 ²Atlantic Oceanographic and Meteorological Laboratory (NOAA/AOML), Miami,
7 Florida

8 ³JISA0/University of Washington and Pacific Marine Environmental Laboratory
9 (NOAA/PMEL), Seattle, Washington

10 ⁴University of Wisconsin at Madison, Department of Atmospheric and Oceanic
11 Sciences, Madison, Wisconsin

The Atlantic Meridional Mode is the dominant source of coupled atmosphere–ocean variability in the tropical Atlantic, characterized by a hemispheric sea surface temperature gradient and cross equatorial surface winds that reinforce ocean temperature anomalies in both hemispheres^{1–4}. The Atlantic Meridional Mode is thermodynamically damped and requires external forcing to persist as is observed³. However, there is not consensus regarding the external forcings that have excited the AMM in the historical record, and thus govern regional coupled climate variability⁴. Here we use observations and a physical model to show that the Atlantic Meridional Mode is excited by variability in African dust outbreaks via the dust radiatively-forced SST anomalies on interannual to decadal time scales. Our analysis suggests that SST anomalies resulting from the aerosol direct effect persist in time via the wind-evaporation-sea surface temperature feedback⁵ that defines the Atlantic Meridional Mode^{1–3}. We conclude that on interannual to decadal time scales the state of the tropical Atlantic is directly tied to land surface processes over West Africa via dust emission. These results suggest that human activity may already be altering regional climate via land use change^{6–8}.

West Africa is the largest global source of atmospheric dust due to an abundance of deflatable materials and strong seasonally varying low-level winds⁹, and the majority of dust generated in West Africa is advected over the tropical and subtropical North Atlantic¹⁰. Mineral aerosols have a high single scatter albedo and over dark surfaces the scattering of sunlight dominates absorption of infrared radiation such that the net effect at the surface is a reduction in downwelling

1 radiation¹¹. To first order such a reduction in the surface heat flux cools the ocean
2 mixed layer^{12–14}, and since the mid 1980s a decrease in Atlantic dust optical
3 depth^{11,15} (Fig 1) has resulted in an increase in the amount of solar radiation
4 absorbed at the ocean surface¹⁴ and a small upward trend in tropical North Atlantic
5 sea surface temperature (SST)¹². Between 1955 and 1985 there was a pronounced
6 increase in dust optical depth over the tropical North Atlantic^{7,11} (Fig 1), in turn
7 cooling SST here⁷.

8 To investigate the impact of DAOD variability on regional climate we first
9 estimate the effect of dust on tropical North Atlantic SST by forcing a version of the
10 Massachusetts Institute of Technology Ocean General Circulation Model^{16,17} with a
11 dust radiative forcing climatology that covers the period 1955–2008¹¹. The change
12 in SST from anomalous dust optical depth is obtained by differencing model output
13 from a 54-year run that is forced only by seasonally varying surface heat fluxes from
14 an atmospheric reanalysis¹⁸, and a separate run in which the monthly fluxes also
15 include the historical contribution to the surface radiative flux by anomalous dust
16 optical depth. We are estimating the effect of dust on Atlantic SST about the
17 climatological mean state, thus from the model experiments periods of anomalously
18 high dust force SST cool anomalies while periods of anomalously low dust loading
19 force SST warm anomalies (see Methods).

20 The spatial structure of the sensitivity of tropical Atlantic SST to changes in
21 dust is estimated via a composite difference of modeled SST during the five most
22 (1983–1988) and least (1956–1958, 2004, 2005) dusty years (Fig 1). The dust
23 forced SST (hereafter ΔSST) composite reaches a maximum of 0.3°C over a broad

region centered on 25°W and 20°N, decays to zero near the equator and slightly north of 30°N, and exhibits a weaker gradient to the west of the cool maximum. The spatial structure of the ΔSST composite is very similar to that of the Atlantic Meridional Mode (AMM) (Fig 1). The AMM structure is estimated via a Maximum Covariance Analysis of tropical Atlantic SST and reanalysis 10-*m* winds over the domain 21°S–32°N and 74°W to the West African coastline². The asymmetric structure of the AMM reflects the meridional gradient feature of the AMM, and the wind-evaporation-SST (WES) feedback, the destabilizing mechanism for transient growth of the AMM^{3,5,19}. The WES feedback is the tendency of surface winds to blow from the cool to the warm hemisphere and reduce (increase) evaporation in the warm (cool) hemisphere via a net weakening (enhancement) of the climatological easterlies, thereby reinforcing the existing SST gradient^{3,5}.

Through the WES feedback, the AMM is strongly influenced by the underlying SST. Therefore, the similarity in the spatial structures of the AMM and ΔSST suggests that dust radiative forcing may excite coupled variability of the equatorial Atlantic. To demonstrate the mechanics of such a process we consider the coupled response to dust-like radiative forcing in the idealized coupled equatorial model³:

$$\frac{\partial}{\partial t} \begin{pmatrix} u \\ v \\ h \\ T \end{pmatrix} = \begin{pmatrix} -\epsilon_u & \beta y & -g' \partial / \partial x & \Gamma_{RG} \partial / \partial x \\ -\beta y & -\epsilon_u & -g' \partial / \partial y & \Gamma_{RG} \partial / \partial y \\ -H_b \partial / \partial x & -H_b \partial / \partial y & -\epsilon_M(y) & 0 \\ \alpha(y) & 0 & 0 & -\epsilon_T + \gamma \nabla^2 \end{pmatrix} \begin{pmatrix} u \\ v \\ h \\ T \end{pmatrix} + \begin{pmatrix} 0 \\ 0 \\ 0 \\ F_{dust} \end{pmatrix} \quad (1)$$

where the left-hand side of (1) are the time tendencies of the zonal (*u*) and meridional (*v*) winds, perturbation boundary layer height (*h*), and SST (*T*). The right hand side of (1) consists of the dynamical system matrix (4x4 matrix) and a forcing

vector indicating possible SST forcing from dust (F_{dust}). The upper-left 3x3 matrix of the dynamical system matrix are the reduced gravity (g') shallow water equations on an equatorial beta plane linearized about a state of rest²⁰, with linear dampening terms along the main diagonal; these represent a tropical atmospheric boundary layer of depth H_b . The atmospheric boundary layer is coupled to a slab ocean via SST-induced hydrostatic pressure perturbations ($\Gamma_{RG}T$). The ocean is coupled to the atmosphere via the WES term (α) such that model growth occurs when u and T anomalies are in phase. T anomalies are damped via the linear and harmonic dampening term, in the lower right-hand corner of the 4x4 matrix. All coefficients have the same values as in Vimont³. A parameterized dust forcing can be applied to the model via the right-most vector in (1). Though a simplified version of the real atmosphere, the model in (1) provides a useful theoretical framework for understanding the response of the coupled tropical system to an idealized forcing.

From the unforced version of (1) the AMM emerges both as the structure exhibiting the maximum transient growth, and a steady response to “optimal forcing” anomalies (Vimont, 2010). To examine the theoretical coupled response to dust-like forcing we impose a forcing term F_{dust} in the SST tendency equation (1) with a spatial structure similar to that from our model experiment (ΔSST , Fig. 1), i.e., zonal and meridional scales of 60° longitude and 30° latitude and centered at 20°N (Fig. 1); note that the model is harmonic in the zonal direction. The model is integrated forward for one year, forced with this idealized heating term for the first four months of the model integration, reflecting the typical time scale of anomalous

1 forcing of SST by dust¹¹. During the remaining 8 months, the model solution evolves
2 via the internal coupled dynamics in the homogeneous version of (1).

3 During months one through four, when the dust heating term is applied, the
4 monthly mean maps of the coupled model SST, surface wind, and boundary layer
5 pressure fields show an equatorward and westward migration of SST anomalies
6 outside of the original forcing region, which are forced by the anomalous westerlies
7 (easterlies) on the equatorward side of the negative (positive) geopotential anomaly
8 that overlies the warm (cool) SST anomaly (Fig. 2). Starting in month four there is
9 an SST anomaly in the southern hemisphere that is opposite in sign to the imposed
10 forcing. This SST signal is the response to the anomalous cross-equatorial flow, and
11 it continues to amplify via coupled dynamical processes for several months after the
12 imposed forcing is turned off (Fig S5). At model month eight, four months after the
13 imposed heating is turned off, there still exists a meridionally asymmetric SST
14 anomaly accompanying the cross-equatorial winds, and this pattern persists
15 through the model integration (Fig S5).

16 The similarity between the spatial structure of the AMM and ΔSST (Fig. 1)
17 and the result from our idealized model experiments (Fig. 2) suggest there may be a
18 coupled equatorial response to Atlantic dust outbreaks in nature. We next
19 investigate the relative importance of such dust-forced variability on interannual to
20 decadal time scales by comparing the time series of the observed AMM with the
21 component of the observed AMM we estimate to be directly forced by dust. We first
22 recover the observed AMM time series (AMM_{obs}) by projecting maps of observed SST
23 anomalies²² onto the stationary spatial pattern of the AMM (Fig 1) ($AMM_{x,y}$), and

1 then normalize the resultant time series to a mean of zero and standard deviation of
 2 one,

$$AMM_{obs}(t = t_0) = \frac{SST'(t = t_0) \times AMM_{x,y}}{\sigma_{AMM(t)}}. \quad (2)$$

3 The left-hand side of (2) indicates the value of AMM_{obs} at time t_0 , the prime indicates
 4 monthly anomalies of SST also at time t_0 , and $\sigma_{AMM(t)}$ is the standard deviation of the
 5 product in the numerator for all t (Fig 2). We note that the SST anomalies have been
 6 detrended and SST variability associated with ENSO has been removed by
 7 regressing out the monthly Nino 3.4 index at each point (although excluding the
 8 ENSO regression step gives a very similar result). We similarly estimate the dust-
 9 forced component of the AMM (AMM_{dust}) by calculating the magnitude of the
 10 projection of monthly mean ΔSST onto $AMM_{x,y}$,

$$AMM_{dust}(t = t_0) = \frac{\Delta SST(t = t_0) \times AMM_{x,y}}{\sigma_{AMM(t)}}, \quad (3)$$

11 where the left-hand side of (3) indicates the value of AMM_{dust} at time t_0 and ΔSST is
 12 used in place of SST' in (2). The normalization coefficients are the same for AMM_{obs}
 13 and AMM_{dust} , thus the magnitudes of the two time series are comparable.

14 AMM_{obs} exhibits both interannual and decadal scale variability^{1,2,19}, with
 15 coherent periods of positive and negative values during each decade (1) (Fig 3a).
 16 AMM_{dust} contains longer periods of coherent positive and negative values, with
 17 mostly positive values during the beginning and end of the record, and mostly
 18 negative values in the middle of the time series, consistent with historical estimates

1 of regional dustiness^{7,11,15} (Fig 3b). AMM_{dust} anomalies are of a similar magnitude to
2 AMM_{obs} . The range of annual mean AMM_{obs} and AMM_{dust} is 5.32 and 3.02 units
3 standard deviation, respectively, and the standard deviation of AMM_{dust} is 0.67 (that
4 of AMM_{obs} is by definition unity). The magnitude and standard deviation of 5-year
5 low pass filtered AMM_{obs} and AMM_{dust} anomalies (Fig. 3C) are nearly equal,
6 suggesting that dust forcing is an important component of observed coupled
7 variability on decadal time scales.

8 Based on our idealized coupled model experiments (Fig. 2) and given time
9 scales of the WES feedback^{3,5} we expect growth of any dust (radiatively) forced
10 AMM anomaly over a finite period. SST forcing by dust should excite a zonal wind
11 anomaly that reinforces and grows the initial radiatively-forced anomaly. The cross-
12 correlation function of the unfiltered and five year low pass filtered AMM_{obs} and
13 AMM_{dust} are a maximum (0.34 and 0.57, respectively) when the dust forced
14 component leads the AMM by two years, both statistically significant at the 95%
15 level based on a 1000-sample permutation test (Fig S6). The positive correlation
16 when AMM_{dust} leads AMM_{obs} suggests that the integrated effect of anomalous dust
17 surface radiative forcing and the WES feedback conspire to amplify the response of
18 the coupled mode to anomalous dust optical depth. Given the time scales of
19 meridional mode growth³ we expect the cross-correlation function to be a
20 maximum when AMM_{dust} leads AMM_{obs} by one year, not the two years shown in our
21 analysis (Fig S6). We speculate the discrepancy is related to uncertainty in the
22 seasonality of the radiative forcing from our annual dust reconstruction, and our use
23 of uncoupled model experiments for estimating the spatial and temporary

1 characteristics of ΔSST , although the neglect of slow ocean processes in the coupled
2 model may also be relevant.

3 Historical variability of the AMM may have been externally forced by the
4 NAO and ENSO²³, and AMO²⁴, or emerged from random variability¹. Historical dust
5 emission is a function of surface processes and local to synoptic scale meteorological
6 conditions^{7,9,10,15}, and transport is related to the phase of the North Atlantic
7 Oscillation²⁵ and ENSO²⁶. We suggest that dust variability contributes to observed
8 AMM variability via the coupled mechanisms described here. Our finding that solar
9 radiation forces a significant portion of the observed tropical Atlantic SST variability
10 is consistent with a tropical Atlantic surface heat budget analysis²⁷ and additional
11 model experiments examining the relative contributions of latent heat and solar
12 radiation fluxes to long-term variability of the AMM (See Supplement).

13 Since tropical Atlantic environmental conditions are more favorable for
14 hurricane genesis and intensification when the AMM is in a positive phase^{24,28}, the
15 negative correlation between Atlantic dustiness and hurricane activity^{29,30} may be
16 the result of forcing of the AMM by anomalous dust outbreaks. In addition,
17 anthropogenic land use has played a role in augmenting African dust emissions,
18 although by what amount is uncertain⁶⁻⁸. Thus the possibility exists that human
19 activity may have already been altering regional climate through the dust-ocean-
20 atmosphere interactions shown here. Furthermore, in the future carbon dioxide
21 fertilization may lead to shrinking desert areas and a reduction in African dust
22 outbreaks⁶, and therefore more favorable conditions for hurricanes to form and
23 intensify via anomalous dust-forcing of the AMM.

1 **Methods**

2 The dust climatology¹¹ is based on a reconstructed time series of dust optical
3 depth over Cape Verde that utilizes a coral proxy record (1955–1994) and satellite
4 retrievals (1982–2008). African dust outbreaks are advected over the Atlantic at the
5 latitude of Cape Verde throughout the year¹⁰, and as such dust optical depth over
6 the tropical North Atlantic is well-correlated to dust at Cape Verde on monthly to
7 interannual time scales¹¹. Additionally, a comparison of the dust time series used
8 here with a slightly shorter series made from in-situ measurements at Barbados¹⁵
9 shows a very high level of agreement on interannual to decadal time scales (Fig S1).
10 Additional details regarding the forcing and dust optical depth climatology are in
11 Evan and Mukhopadhyay¹¹. A global version of the Massachusetts Institute of
12 Technology Ocean General Circulation Model^{16,17} is spun up to a steady state with
13 climatological monthly surface horizontal momentum fluxes and surface heat fluxes
14 calculated offline using the National Centers for Environmental Protection
15 Reanalysis¹⁸. We performed two separate model runs, each initialized from a 150
16 year spinup run. For the control run we continue forward the climatology forcing for
17 an additional 54 years, for the perturbation run we subtract from the surface heat
18 flux climatology the monthly mean contribution from anomalous dust variability.
19 The dust contribution to the surface heat flux is defined as the monthly dust aerosol
20 direct effect at the surface minus the annual cycle. The difference between the
21 control and perturbation runs is considered to be the effect of departures in
22 dustiness from the seasonal mean. Additional details on the model configuration can
23 be found in the supplemental material.

References

1. Chang, P., L. Ji & H. Li A decadal climate variation in the tropical Atlantic Ocean from thermodynamic air-sea interactions. *Nature* **385**, 516–518 (1997)
2. Chiang, J. C. H. & D. J. Vimont Analogous Pacific and Atlantic Meridional Modes of tropical atmosphere-ocean variability. *J. Clim.* **17**, 4143–4158 (2004)
3. Vimont, D. J. Transient Growth of thermodynamically coupled variations in the tropics under an equatorially symmetric mean state. *J. Clim.* **23**, 5771–5789 (2010)
4. Xie, S.-P. & J. A. Carton Tropical Atlantic variability: Patterns, mechanisms, and impacts, in Earth's Climate: The Ocean-Atmosphere Interaction, *Geophys. Monogr. Ser.*, vol. 147, edited by C. Wang, S.-P. Xie, and J. A. Carton, pp. 121– 142, AGU, Washington, D. C. (2004)
5. Xie, S.-P. & S. G. H. Philander A coupled ocean-atmosphere model of relevance to the ITCZ in the eastern Pacific. *Tellus, Ser. A* **46**, 340–350 (1994)
6. Mahowald, N. M. Anthropocene changes in desert area: Sensitivity to climate model predictions. *Geophys. Res. Lett.* **34**, L18817, doi:10.1029/2007GL030472 (2007)
7. Mahowald, N. M., *et al.* Observed 20th century desert dust variability: impact on climate and biogeochemistry. *Atmos. Chem. Phys. Discuss.* **10(5)**, 12585–12628 10.5194/acpd 10 12585 (2010)
8. Mulitza, S. *et al.* Increase in African dust flux at the onset of commercial agriculture in the Sahel region. *Nature* **466**, 226–228 (2010)

- 1 9. Goudie, A. S. & N. J. Middleton *Desert Dust in the Global System*. Springer, New York.
2 (2006)
- 3 10. Kaufman, Y. J. *et al.* Dust transport and deposition observed from the Terra-
4 Moderate Resolution Imaging Spectroradiometer (MODIS) spacecraft over the
5 Atlantic Ocean. *J. Geophys. Res.* **110**, D10S12, doi:10.1029/2003JD004436 (2005)
- 6 11. Evan, A. T. & S. Mukhopadhyay African Dust over the Northern Tropical Atlantic:
7 1955–2008. *J. Appl. Meteor. Climatol.* **49**, 2213–2229 (2010)
- 8 12. Evan, A. T., D. J. Vimont, A. K. Heidinger, J. P. Kossin & R. Bennartz The role of
9 aerosols in the evolution of tropical North Atlantic Ocean temperature anomalies.
10 *Science* **324**, 778–781, doi:10.1126/Science.1167404 (2009)
- 11 13. Foltz, G. R. & M. J. McPhaden Impact of Saharan dust on tropical North Atlantic
12 SST. *J. Climate* **21**, 5048–5060. (2008)
- 13 14. Foltz, G. R. & M. J. McPhaden Trends in Saharan dust and tropical Atlantic climate
14 during 1980–2006. *Geophys. Res. Lett.* **35**, L20706, doi:10.1029/2008GL035042
15 (2008)
- 16 15. Prospero, J. M. & P. J. Lamb African droughts and dust transport to the
17 Caribbean: Climate change implications. *Science* **302**, 1024–1027 (2003)
- 18 16. Marshall, J., A. Adcroft, C. Hill, L. Perelman & C. Heisey A finite-volume,
19 incompressible Navier Stokes model for studies of the ocean on parallel computers. *J.*
20 *Geophys. Res. -Oceans* **102**, 5753–5766 (1997)

- 1 17. Marshall, J., C. Hill, L. Perelman & A. Adcroft Hydrostatic, quasi-hydrostatic, and
2 nonhydrostatic ocean modeling. *J. Geophys. Res. -Oceans* **102**, 5733–5752 (1997)
- 3 18. Kalnay, E. et al. The NCEP/NCAR 40-Year Reanalysis Project. *Bull. Am. Meteorol.*
4 *Soc.* **77**, 437–471. (1996)
- 5 19. Chang, P., L. Ji & R. Saravanan A Hybrid Coupled Model Study of Tropical Atlantic
6 Variability. *J. Climate* **14**, 361–390 (2001)
- 7 20. Battisti, D. S., E. S. Sarachik, and A. C. Hirst, A consistent model for the large-scale
8 steady atmospheric circulation in the tropics. *J. Climate*, **12**, 2956–2964 (1999)
- 9 22. Rayner, N. A. *et al.* Global analyses of sea surface temperature, sea ice, and night
10 marine air temperature since the late nineteenth century. *J. Geophys. Res.* **108**, 4407,
11 doi:10.1029/2002JD002670 (2003)
- 12 23. Czaja, A., P. van der Vaart, and J. Marshall A diagnostic study of the role of remote
13 forcing in tropical Atlantic variability. *J. Climate*, **15**, 3280–3290 (2002)
- 14 24. Vimont, D. J. & J. P. Kossin The Atlantic meridional mode and hurricane activity.
15 *Geophys. Res. Lett.* **34**, L07709, doi:10.1029/2006GL029683 (2007)
- 16 25. Moulin, C., C. Lambert, F. Dulac, & U. Dayan Control of atmospheric export of dust
17 from North Africa by the North Atlantic Oscillation. *Nature* **387**, 691–694 (1997)
- 18 26. Evan, A. T., Heidinger, A. K. & Knippertz, P. Analysis of winter dust activity off
19 the coast of West Africa using a new 24-year over-water advanced very high
20 resolution radiometer satellite dust climatology. *J. Geophys. Res.*, **111**, D12210,
21 doi:10.1029/2005JD006336 (2006)

- 1 27. Foltz, G.R., and M.J. McPhaden, 2006: The role of oceanic heat advection in the
2 evolution of tropical North and South Atlantic SST anomalies. *J. Climate*, 19, 6122-
3 6138.
- 4 28. Kossin, J. P. & D. J. Vimont A more general framework for understanding Atlantic
5 hurricane variability and trends. *Bull. Amer. Meteor. Soc.* **88**, 1767-1781 (2007)
- 6 29. Evan, A. T., J. Dunion, J. A. Foley, A. K. Heidinger & C. S. Velden New evidence for a
7 relationship between Atlantic tropical cyclone activity and African dust outbreaks.
8 *Geophys. Res. Lett.* **33**, L19813, doi:10.1029/2006GL026408 (2006)
- 9 30. Evan, A. T. *et al.* Ocean temperature forcing by aerosols across the Atlantic
10 tropical cyclone development region. *Geochem. Geophys. Geosyst.* **9**, Q05V04,
11 doi:10.1029/2007GC001774 (2008)

12 **Corresponding author**

13 Correspondence to: Amato T. Evan, ate9c@virginia.edu

14 **Acknowledgements**

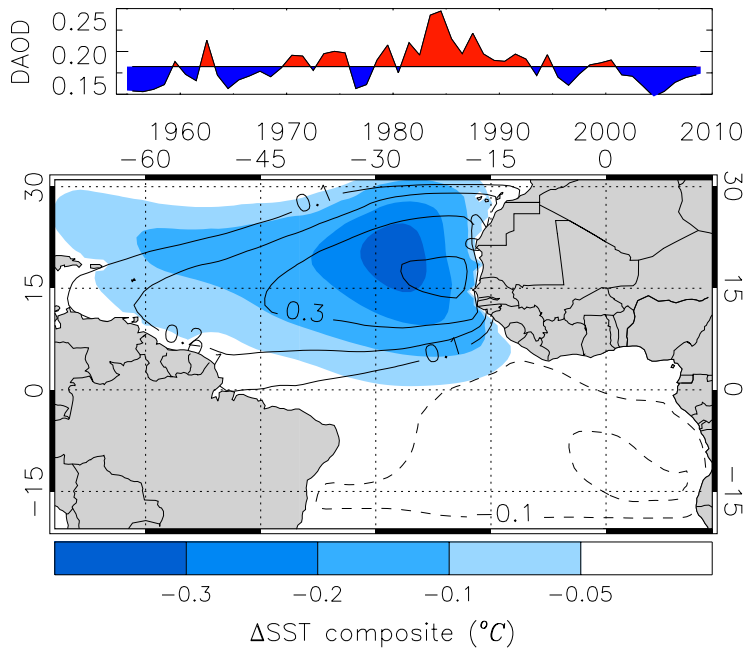
15 Funding for this work was provided by NOAA/CLIVAR grants NA10OAR4310136
16 and NA10OAR4310207.

17 **Author Contributions**

18 A.T.E. and D.J.V. designed and performed the model experiments; A.T.E, G.R.F., D.J.V.
19 and D.Z. analyzed and interpreted the model output and co-wrote the paper.

20

1 **Figures**



2

3 **Figure 1. Time series of dust optical depth, footprint of dust on tropical**

4 **Atlantic SST, and the spatial pattern of the AMM.** Plotted is the annual time series

5 of dust optical depth (DAOD)¹⁶ averaged over the region 10-20°N and 20°-50°W

6 (top). Dust optical depth is a measure of the extinction of light through the dust

7 layer and is proportional to mass concentration. In the map are contours of the

8 spatial pattern of the AMM (AMM_{x,y}), defined as the regression of SST (°C) onto the

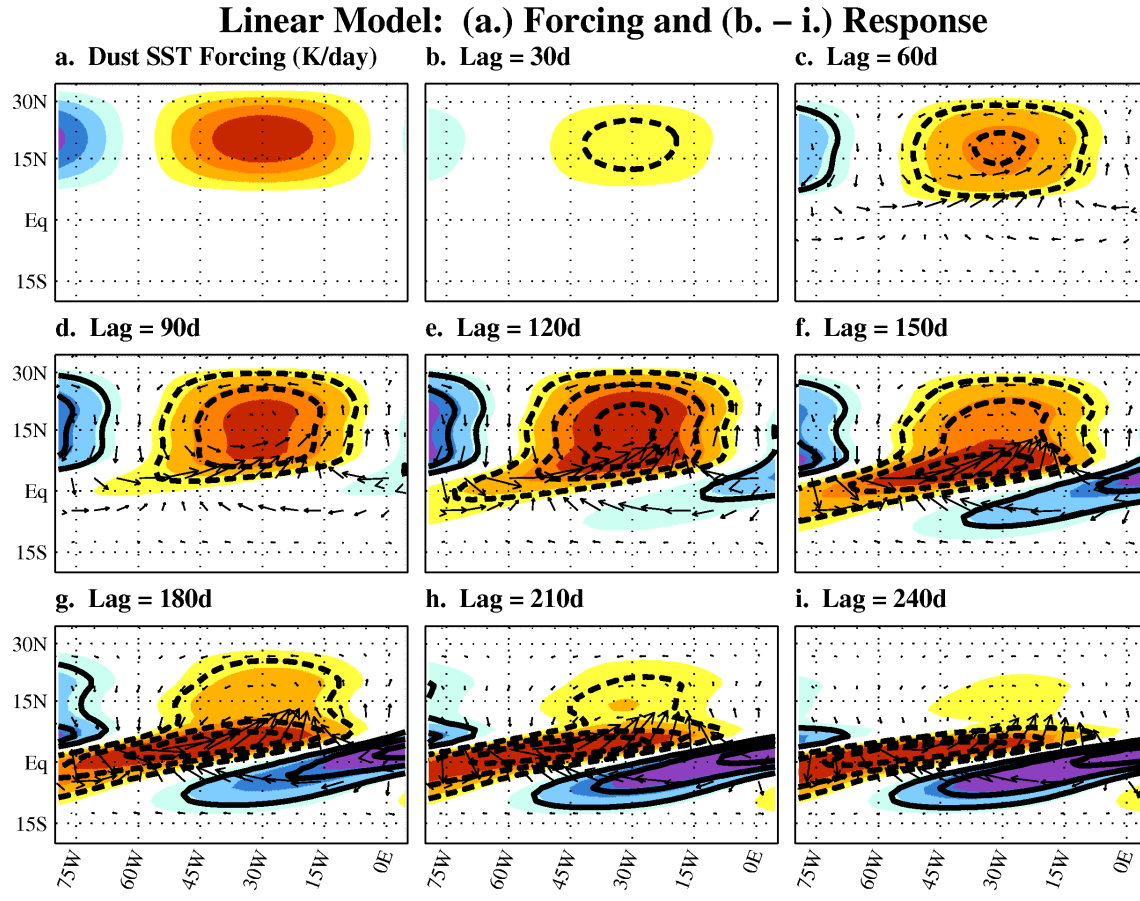
9 leading mode of a maximum covariance analysis applied to reanalysis SST and

10 lower-level winds over the domain 19°S–30.5°N and 71°W–13°E². Shading denotes

11 composite differences of ΔSST and demonstrates the similarity between the AMM

12 spatial pattern and the SST pattern forced by changes in dust optical depth.

1



2

3 **Figure 2. Monthly mean output from idealized coupled model experiments.**

4 The top left panel (a.) depicts the idealized dust forcing (K day^{-1}) used to force the

5 coupled model during the first four months. The remaining panels (b. – i.) show the

6 equatorward and westward evolution of the model response in monthly mean SST

7 (shaded), boundary layer pressure (contours), and boundary layer winds (vectors)

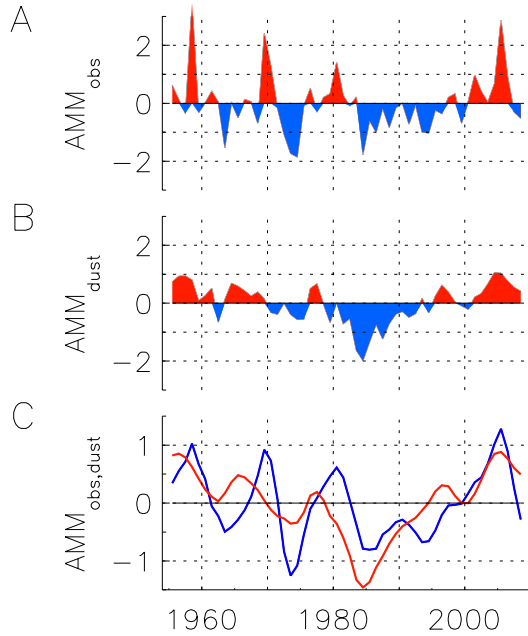
8 for model months 1-8. Positive (negative) SST anomalies are shaded red (blue) and

9 positive (negative) pressure anomalies are drawn with solid (dashed) contours and

10 the zero line has been omitted. Units are arbitrary but consistent throughout panels

11 (b.) – (i.) so amplitudes may be compared. For reference, a 5 W m^{-2} forcing in panel

- 1 (a.) would produce a maximum warming of about 0.2 K in four months (panel e.).



1

2 **Figure 3. Observed and dust-forced component of the AMM time series.** Plotted

3 are annually averaged observed AMM time series (A), annually averaged dust-

4 forced component of the AMM (B), and the 5-year low-pass filtered AMM_{obs} (blue)

5 and AMM_{dust} (red) time series (C). As both time series have the same normalization,

6 similarity between AMM_{obs} and AMM_{dust} indicates the magnitude of direct forcing of

7 the AMM by African dust outbreaks.

8